Applied Catalysis B: Environmental 140–141 (2013) 276–282

Contents lists available at SciVerse ScienceDirect

Applied Catalysis B: Environmental

journal homepage: www.elsevier.com/locate/apcatb

The effect of SiO_2 on a novel CeO_2–WO_3/TiO_2 catalyst for the selective catalytic reduction of NO with NH_3

Yue Peng, Caixia Liu, Xueying Zhang, Junhua Li*

State Key Joint Laboratory of Environment Simulation and Pollution Control, School of Environment, Tsinghua University, Beijing 100084, China

ARTICLE INFO

Article history:
Received 20 January 2013
Received in revised form 13 April 2013
Accepted 14 April 2013
Available online 20 April 2013

Keywords:
$DeNO_x$
Selective catalytic reduction
SiO_2
CeO_2
WO_3

ABSTRACT

A series of novel catalyst complexes for the selective catalytic reduction of NO_x to NH_3 were prepared by doping CeO_2–WO_3/TiO_2 with different loadings of SiO_2. The complexes were synthesized by impregnating P25 with colloidal silica to form a complex support. The NO_x conversion values and the calculated reactive rate constants confirm that the presence of SiO_2 increased the reaction activity at low temperatures. This increase in activity may be directly correlated to the increase in the presence of unstable Brønsted acid sites as well as active nitrite, monodentate nitrates and adsorbed NO_2, as opposed to an increase in the BET surface area and a change in the redox properties. Furthermore, the surface bridging and bidentate nitrate species that originated from the adsorption of NO_x were quite stable and inactive below 300 °C. Finally, both Ti(1)Si(0) and Ti(3)Si(1) catalysts were employed to study the reaction mechanism by in situ IR spectroscopy at 200 °C. The two catalysts exhibited similar reaction mechanisms, wherein the Lewis and Brønsted acid sites reacted with active nitrite, monodentate nitrates and adsorbed NO_2 species.

1. Introduction

Nitrogen oxide species (NO_x) emitted from automobile exhaust gas and the industrial combustion of fossil fuels are major air pollutants. The selective catalytic reduction (SCR) of NO_x to form NH_3 is an effective technique for the reduction of NO_x from diesel exhaust or coal-fired power plants. In industry, the most widely employed SCR catalyst is V_2O_5–WO_3/TiO_2, which is effective in a relatively narrow temperature window of 300–400 °C [1,2]. Despite its widespread use, several problems have been associated with this catalyst system: the environmental toxicity of vanadium species, the high activity for the oxidation of SO_2 to SO_3, and the low N_2 selectivity at high temperatures due to N_2O formation [3,4]. Therefore, many researchers are working on developing new catalysts to avoid the challenges discussed above.

Recently, catalysts without vanadium have been extensively studied, such as transition metal Fe, Mn and Cu oxides supported on TiO_2 or ZrO_2 [3,5–7], as well as Fe and Cu exchanged zeolites [8,9]. Moreover, as an important catalyst support, ceria and ceria-containing materials have been widely applied as co-catalysts or structural promoters of heterogeneous catalytic reactions because of their excellent reducibility and remarkable oxygen storage capability [10]. Qi et al. [11] developed MnO_x–CeO_2 catalysts by different synthetic methods and obtained catalysts with favorable activities for NO_x reduction at low temperature. Wu et al. [12] compared the SCR performance of Mn–Ce catalysts supported on TiO_2 and Al_2O_3. The results demonstrated that different styles of acid sites (Lewis acidity predominant on Mn–Ce/Ti and Brønsted acidity major on Mn–Ce/Al) were responsible for the different activity regions and reaction mechanisms. He et al. [13] investigated the SO_2 deactivation on Ce/TiO_2 catalyst and its stability in the presence of H_2O, CO_2 and C_3H_6 [14]. In our previous studies [15–18], the CeO_2–WO_3 or CeO_2–WO_3/TiO_2 (Ce–W/Ti) catalysts exhibited favorable SCR performance above 200 °C and increased the activity window of the traditional V_2O_5–WO_3/TiO_2. In addition, this system exhibited better resistance to SO_2 and alkali metals at high temperatures. However, the synthetic methods for the preparation of these catalysts involve either co-precipitation or sol–gel reactions, which are not favorable for industrial catalyst preparation. As a structural promoter, SiO_2 mixed with TiO_2 for vanadia based catalysts is a common method in industry owing to its large BET surface area, remarkable surface acidity and structural strength of SCR monolith catalyst. At the same time, studies on the chemical tuning of the non-vanadium based catalysts are quite rare [19–21]. To improve the applicability of this Ce–W/Ti catalyst, it is necessary to investigate the effect of SiO_2 on Ce–W/Ti catalysts.

This paper investigates the influences of SiO_2 on the Ce–W/Ti catalyst prepared with different Ti to Si ratios using the industrially relevant impregnation method. For this purpose, both the physical and chemical characteristics of Ce–W/Ti–Si catalysts and their SCR performance under a high gas hourly space velocity (GHSV) were investigated.

* Corresponding author. Tel.: +86 10 62771093.
E-mail address: lijunhua@tsinghua.edu.cn (J. Li).

0926-3373/$ – see front matter © 2013 Elsevier B.V. All rights reserved.
http://dx.doi.org/10.1016/j.apcatb.2013.04.030

2. Experimental

2.1. Catalyst preparation

The traditional and SiO_2 doped catalysts were prepared by the impregnation method. Specific amounts of ammonium paratungstate and cerium nitrate were mixed in an oxalic acid solution followed by the impregnation of specific amounts of TiO_2 (P25) and SiO_2 (30 wt% colloidal silica, Aldrich). The mixture was stirred for 2 h, dried overnight at 120 °C and then calcined at 500 °C for 5 h in static air. The active component of CeO_2 and WO_3 was 10 wt%. A catalyst denoted as Ti(x)Si(y) indicates that the mass ratio of TiO_2 and SiO_2 is x:y.

2.2. Catalytic performance

Activity measurements were performed in a fixed-bed quartz reactor (inner diameter 9 mm) using 100 mg of catalyst with a 40–60 mesh. The feed gas mixture contained 500 ppm NO, 500 ppm NH_3 (500 ppm SO_2 when employed), 3% O_2, and the balance of N_2. The total flow rate of the feed gas was 200 cm^3/min and the GHSV was approximately 120,000 $cm^3\ g^{-1}\ h^{-1}$. The concentrations of inlet and outlet gases were continually monitored by an FTIR spectrometer (Gasmet DX-4000). Activity data were recorded when the reaction reached a steady state after 30 min at each temperature.

To further evaluate the catalytic activity, kinetic parameters for the NO conversion were calculated according to the following equation:

$$k = -\frac{V}{W} \times \ln(1 - x) \quad (1)$$

where k is the reaction rate constant ($cm^3\ g^{-1}\ s^{-1}$), V is the total gas flow rate ($cm^3\ s^{-1}$), W is the mass of catalysts in the reactor, and x is subscript in NO_x. The equation is based on the theory that the reaction is first-order with respect to NO and zero-order with respect to NH_3 [2].

2.3. Catalyst characterization

The BET surface area of the samples was evaluated using a Micromeritics ASAP 2020 apparatus. The crystal structure was determined using an X-ray diffractometer (XRD) (Rigaku, D/max-2200/PC) operating at 30 kV and 30 mA using CuKα radiation. The structure of WO_3 was examined by micro-Raman spectroscopy (Renisaw, InVia) under the excitation with a 532 nm^{-1} laser.

The temperature-programmed desorption (TPD) of NH_3 or NO ($NO + O_2$) was performed using a chemisorption analyzer (Micromeritics, ChemiSorb 2720 TPx). For temperature-programmed reduction of H_2, the sample was placed under a 10% H_2/Ar gas flow at a rate of 10 °C/min up to 900 °C; for TPD, the sample first exposed on a 500 ppm NH_3/He (NO/He) gas flow for 1 h, allowed to undergo isothermal desorption under He for 30 min, and then desorbed under a He gas flow at a rate of 10 °C/min up to 600 °C. The gas flow was set to 50 cm^3/min. Each sample was pre-treated at 300 °C in He for 1 h prior to testing.

In situ DRIFTS spectra were recorded on a Fourier transform infrared spectrometer (FTIR, Nicolet NEXUS 870) equipped with a SMART collector and an MCT detector cooled by liquid N_2. Diffuse reflectance measurements were performed in situ in a high temperature cell equipped with a ZnSe window. The catalyst was heated to 350 °C under N_2 at a total flow rate of 100 cm^3/min for 1 h to remove any adsorbed impurities. The background spectrum was recorded in a flowing N_2 atmosphere and was subtracted from the sample spectra. The DRIFTS spectra were recorded by accumulating 100 scans with a resolution of 4 cm^{-1}.

3. Results and discussion

3.1. Characterization of the catalysts

The BET surface areas of Ti(x)Si(y) catalysts prepared using different Ti:Si ratios as well as their corresponding pore volumes and average pore diameters are provided in Table 1. With increasing SiO_2 to Ti ratio, a remarkable increase in the BET surface area and the pore volume were observed, whereas the average pore diameters remained nearly unchanged. The XRD patterns of the Ti(x)Si(y) catalysts are provided in Fig. 1(a). The increase in SiO_2 loadings did not influence the peak locations or the phase transition from anatase to rutile of TiO_2; rather, they reduced the main peak intensity of TiO_2 anatase (1 0 1), corresponding to a decrease in the lower crystallinity of TiO_2. Furthermore, the weak cubic fluorite phase of CeO_2 (1 1 1) can also be observed in the catalysts.

Due to the weak Raman signals of SiO_2 and strong TiO_2 and CeO_2 Raman signals at relatively low wavenumber (less than 700 cm^{-1}), it is possible to obtain structural information about the WO_3 component by the Raman spectroscopy. The results are provided in Fig. 1(b). The peak located at 794 cm^{-1} is attributed to the microcrystalline WO_3 bonds and the shoulder centered at 992 cm^{-1} is due to the W=O stretching mode [22]. With increasing SiO_2 content, the peak at 794 cm^{-1} remains present in all samples with the exception of the Ti(0)Si(1) sample. In contrast, the shoulder associated with this peak exhibits a blue shift to a lower wavenumber, which may be indicative of a slight increase in the W=O bond length at high SiO_2 loadings or an increase in BET surface area. The results indicate that doping with SiO_2 does not significantly distort the surface structure of WO_3. For the Ti(0)Si(1) catalyst, the peak at 794 cm^{-1} disappeared and was replaced by a new peak at 955 cm^{-1} (amorphous WO_3). Similar results have been proposed by Xia et al. who have studied the surface and catalytic properties of WO_3/TiO_2 catalysts [23]. They propose that the main WO_x species present in SiO_2 calcined at 500 °C include amorphous WO_3, in which the W—O—Si bonds played a key role in promoting the oxidation reaction. Overall, these results confirm that doping with SiO_2 increases the BET surface area of the catalysts, enhancing the dispersions of active component WO_x species rather than varying the phase structures of CeO_2 on a TiO_2 support.

3.2. Catalytic activity

Fig. 2 illustrates the SCR activity of Ti(x)Si(y) catalysts prepared using different Ti:Si ratios under a relatively high GHSV of

Table 1
BET surface area (S_{BET}), pore volume (V_P), average pore diameter (D_P), reaction rate constant (k) at 200 °C and Lewis and Brønsted acidities at 100 °C.

	S_{BET} (m^2/g)	V_P (cc/g)	D_P (nm)	k ($cm^3\ g^{-1}\ s^{-1}$)	$10k/S_{BET}$ ($cm^3\ m^{-2}\ s^{-1}$)	Lewis acidity	Brønsted acidity
Ti(1)Si(0)	54.3	0.23	12.5	3.19	0.59	6.01	5.03
Ti(3)Si(1)	85.3	0.47	13.0	14.38	1.68	2.59	9.42
Ti(1)Si(1)	100.4	0.59	12.6	8.43	0.84	1.99	10.68
Ti(1)Si(3)	160.5	0.58	12.6	7.65	0.48	1.76	11.33
Ti(0)Si(1)	159.4	0.55	12.5	5.40	0.34	2.29	12.61

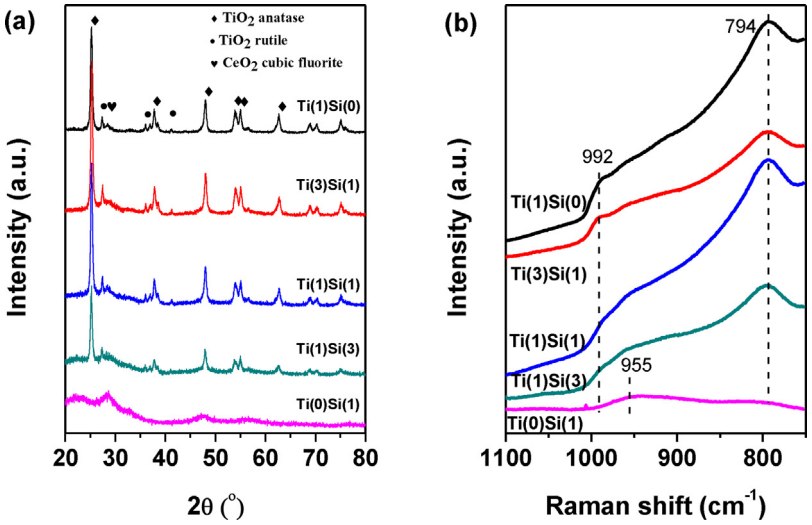

Fig. 1. (a) XRD profiles and (b) Raman spectra of the Ti(x)Si(y) (CeO_2–WO_3/TiO_2–SiO_2) catalysts.

120,000 $cm^3\ g^{-1}\ h^{-1}$. Doping with SiO_2 improved the NO_x conversion below 300 °C, resulting in the following activity sequence: Ti(3)Si(1) > Ti(1)Si(1) > Ti(1)Si(3) > Ti(0)Si(1) > Ti(1)Si(0) at 250 °C. However, when the temperature increased above 400 °C, the Si-containing catalysts exhibited low activity compared with Ti(1)Si(0). The results reveal that SiO_2 enhances the NO_x conversion of Ce–W/Ti catalyst at medium or low temperatures. At the elevated temperature region, doping with SiO_2 suppresses the activity of SCR reaction. An earlier study of V_2O_5/TiO_2–SiO_2 by Kobayashi et al. also reported similar conclusions [19]. The authors attributed this high temperature inhibition effect to the dispersion of vanadia on the support. In this study, the activities of Ti(x)Si(y) under 60,000 $cm^3\ g^{-1}\ h^{-1}$ were tested and the profiles (shown in the supporting information (SI)) exhibit a similar pattern from 150 to 450 °C. Among the SiO_2-containing catalysts, the Ti(3)Si(1) catalyst exhibited the highest SCR activity and the broadest reactivity window. In addition, NH_3 conversion and the selectivity to N_2 were also examined in this study (Figure S2), and the results reveal that no N_2O was detected.

The reaction rate constant k was calculated for the catalysts at 200 °C (Table 1) based on the equation 1, which excludes the influence of mass and heat transfer, where the NO conversion was below 40%. Doping with SiO_2 enhanced the SCR activity and Si-rich catalysts exhibited lower NO_x reduction than Ti-rich catalysts, where the Ti(3)Si(1) catalyst exhibited the highest reaction rate. The influence of the BET surface area was taken into account by calculating the per area (k/S_{BET}) constants. The constant for the Ti(1)Si(0) catalyst was less than that of Ti(3)Si(1) and Ti(1)Si(1) catalysts but greater than the Ti(1)Si(3) and the Ti(0)Si(1) samples.

For the Ti(3)Si(1), the GHSV tolerance as well as the SO_2 and H_2O resistance are shown in Fig. 3. The SCR activity of the catalysts decreased when the GHSV increased from 60,000 to 500,000 $cm^3\ g^{-1}\ h^{-1}$. The highest activity region was between 300

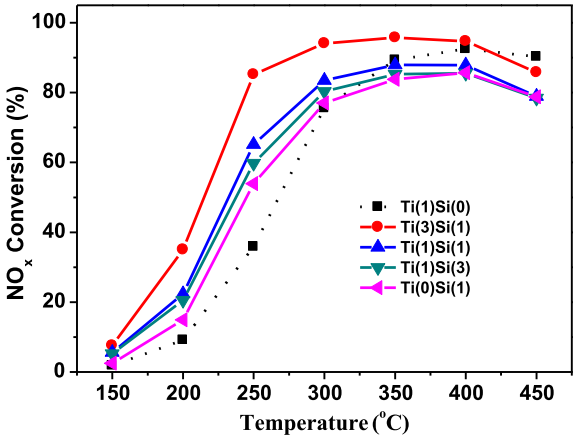

Fig. 2. The SCR performance of Ti(x)Si(y) catalysts. Reaction conditions: catalyst = 100 mg, [NO] = [NH_3] = 500 ppm, [O_2] = 3%, total flow rate = 200 cm^3/min, GHSV = 120,000 $cm^3\ g^{-1}\ h^{-1}$.

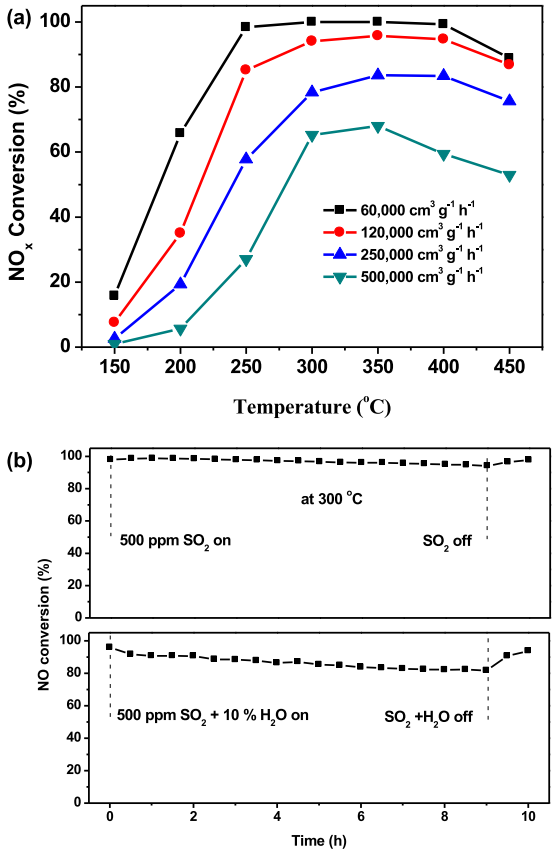

Fig. 3. (a) The NO_x conversion of Ti(3)Si(1) catalyst under different GHSV conditions. (b) The SO_2 and H_2O durability of the Ti(3)Si(1) catalyst at 300 °C under 120,000 $cm^3\ g^{-1}\ h^{-1}$.

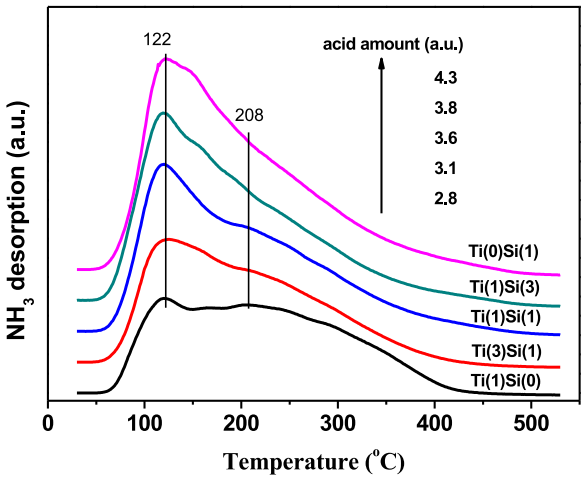

Fig. 4. NH_3–TPD profiles of Ti(x)Si(y) catalysts.

and 350 °C, wherein approximately 70% of NO_x was reduced at 350 °C even under 500,000 $cm^3\ g^{-1}\ h^{-1}$. The SO_2 resistance is carried out for 10 h at 300 °C with 500 ppm SO_2 induced to the gas flow [24]. The results reveal that the Ti(3)Si(1) catalyst exhibited a favorable SO_2 tolerance at 300 °C, at which point the SCR activity decreased slightly. As soon as the SO_2 was shut down, the activity recovered to a sulfur-free scenario within 10 min. When both SO_2 and H_2O were introduced into the reactor, approximately 90% of NO_x conversion was preserved within the first 2 h, and then the activity gradually decreased with the time. Similar conclusions can also be drawn from previous studies on CeO_2–WO_3/TiO_2 catalyst [24], wherein the loss in activity was attributed to the deposition of ammonium sulfate on the surface of the catalyst [14].

3.3. Surface acidity

The redox properties of the Ti(x)Si(y) catalysts were examined using H_2–TPR experiment (Figure S3). The results do not reveal significant differences between the catalysts. Similar findings were also observed by Galan-Fereres et al. [25]. Thus, changes in surface acidity and NO_x species in the presence of SiO_2 might be critical factors during the SCR process. The effect of the amount and strength of the acid on the activity of the catalysts in NH_3–TPD experiments is illustrated in Fig. 4. Two peaks, observed at approximately 122 °C and 206 °C, can be attributed to the weak and strong acid sites for the Ti(x)Si(y) catalysts, respectively. The integral peak area (labeled in the figure) of each catalyst, which correspond to the total acidity, increased with increasing SiO_2 loading. These results suggest that the addition of SiO_2 to TiO_2 may increase the amount of acid but does not influence the strength of the acid (as confirmed by the temperature of desorption peak).

To further distinguish between the different acid types (Lewis or Brønsted acid sites on the catalytic surfaces), in situ DRIFTS experiments were employed to study the NH_3 adsorption/desorption behavior of the catalysts. The NH_3 adsorption on the Ti(x)Si(y) catalysts at 100 °C is shown in Fig. 5(a). The bands at 1148 (1315) and 1573 cm^{-1} can be attributed to the Lewis acid sites, whereas the band at 1448 cm^{-1} can be assigned to the Brønsted acid sites [26]. A broad band in the range 3000–3500 cm^{-1} were observed in the spectrum due to contributions from ν_{as}(N–H), ν_s(N–H), $2\delta_{as}$(H–N–H), $2\delta_s$(H–N–H) and δ_{as}(H–N–H) modes of ammonia adsorbed on the Lewis acid sites [27,28]. The Lewis and Brønsted acidities were obtained by calculating the areas in the DRIFTS spectra at 100 °C. In the presence of SiO_2, the peak at 1148 cm^{-1} disappeared, whereas a peak at 1315 cm^{-1} was observed, which increased in intensity with loading. The peak at 1448 cm^{-1} also

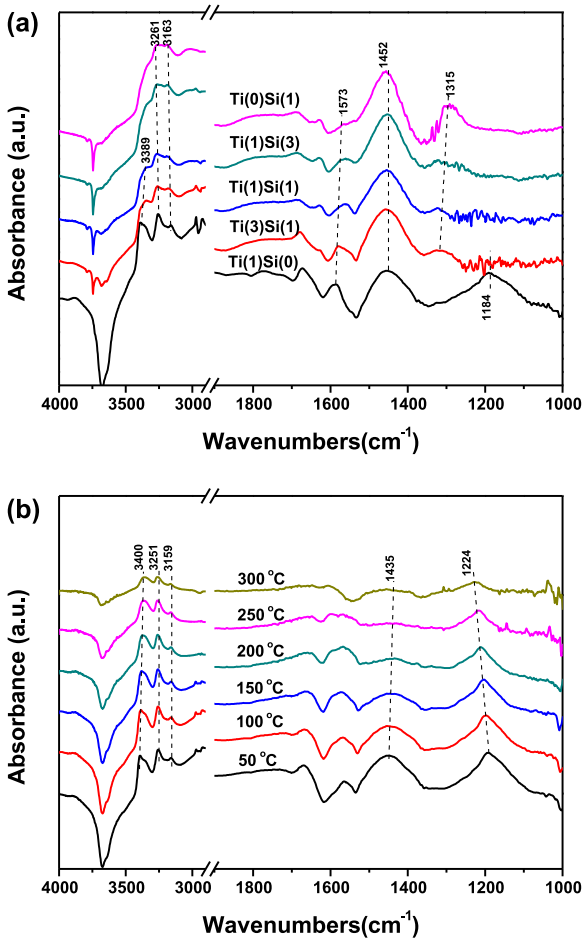

Fig. 5. DRIFTS spectra of (a) the NH_3 adsorption of Ti(x)Si(y) catalysts at 100 °C and (b) the NH_3 desorption of the Ti(1)Si(0) catalyst at the temperature range of 50–300 °C.

increased in intensity with increasing SiO_2 loadings. These results indicate that doping with SiO_2 results in a significant increase in the amount of Brønsted acid sites as well as the nature of the acidity (Lewis/Brønsted). To further investigate the acid strength, NH_3 desorption was performed on the Ti(1)Si(0) sample in the temperature range of 50–300 °C (Fig. 5(b)). Both peak intensities due to Lewis and Brønsted acid sites decreased with the temperature, and the Brønsted acid sites exhibited lower stability compared with the Lewis acid sites: the band at 1448 cm^{-1} nearly disappeared at 300 °C, whereas the band at 1224 cm^{-1} could be still observed. Combined with the NH_3–TPD experiments, the results reveal that SiO_2 enhances surface acidity of the catalysts, especially the number of Brønsted acid sites. In other words, more hydroxyl groups are formed on the surface of the catalyst in the presence of SiO_2. Moreover, the stability of the Brønsted acid sites was lower than that of the Lewis acid site, which could be a possible reason for the low activity of Si-rich catalysts at high temperatures.

3.4. NO_x adsorption

According to the previous studies [29], the oxidation of NO to NO_2 may be the rate-determining step in the SCR of ceria catalysts employed at low temperatures. Tronconi et al. [30,31] referred to the promotion mechanism of NO_2 between 200 and 300 °C as "fast-SCR", and performed extensive studies on the reaction mechanisms and roles of NO_2. To investigate the influence of SiO_2 on the NO_x adsorption/desorption of the catalyst, NO–TPD experiments were performed on the Ti(x)Si(y) samples; the results are provided

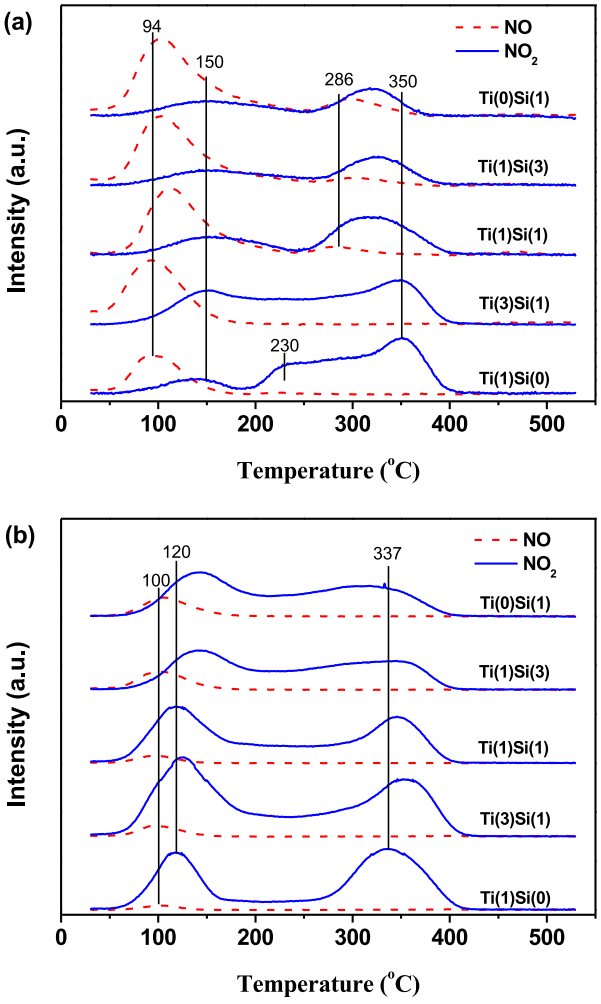

Fig. 6. (a) NO–TPD and (b) NO + O_2–TPD profiles of Ti(x)Si(y) catalysts.

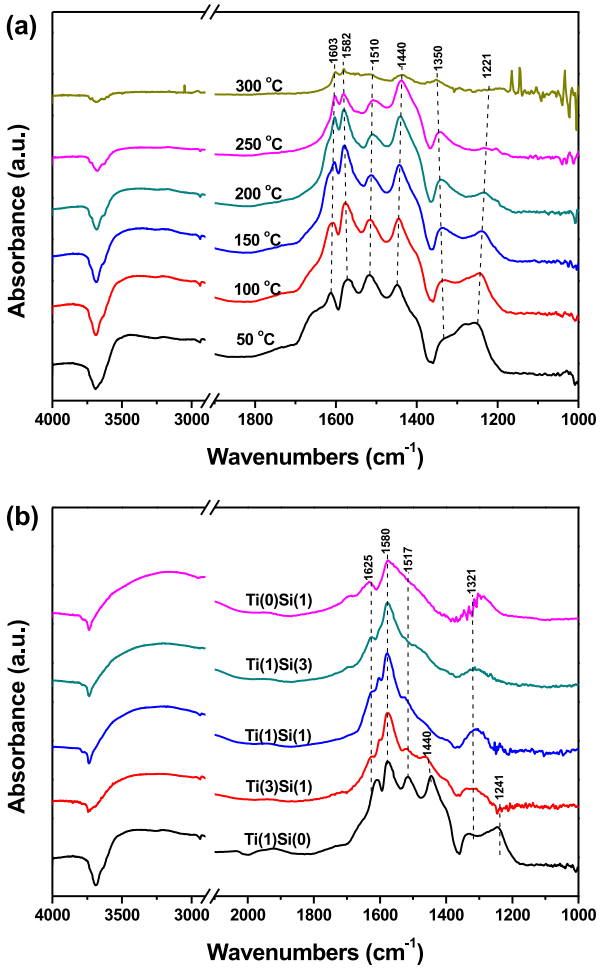

Fig. 7. DRIFTS spectra of (a) the NO_x desorption of the Ti(1)Si(0) catalyst in the temperature range of 50–300 °C and (b) the NO_x adsorption of Ti(x)Si(y) catalysts at 100 °C.

in Fig. 6(a). All the samples exhibited large NO desorption peaks at approximately 100 °C, which can be attributed to the presence of nitrites on the catalytic surfaces [15]. The Si-containing catalysts exhibited higher NO desorption than the Ti(1)Si(0) catalyst, and the amount of desorbed NO also increased with SiO_2 content. The results indicate that the existence of SiO_2 could promote the surface nitrite formation of the catalysts. In the NO_2 desorption profiles of Ti(1)Si(0) and Ti(3)Si(1), two peaks were observed at 150 and 350 °C, as well as a shoulder at approximately 230 °C for the Ti(1)Si(0) sample. In contrast, all other Ti(x)Si(y) catalysts exhibited only a peak at 330 °C, which decreased with increasing SiO_2 loading. These peaks can be attributed to nitrate species wherein the N atom of the oxidized NO_2 bonds with the surface of the O atom (monodentate nitrate) or when the N atom of NO bonds with the surface adjacent to the O atoms (bridging or bidentate nitrate) [15,26]. By correlating the NO_x species assignments with the activity profiles and apparent rate constants, the increased amount of surface nitrite and nitrate species corresponds with an increase in the rate constants, which suggests that the nitrite or nitrate species might be reactive during the SCR process.

Furthermore, NO + O_2–TPD experiments are performed (Fig. 6(b)) to study the oxidation activity for the conversion of NO to NO_2 on the Ti(x)Si(y) catalysts. The results reveal that the NO_2 desorption peak areas followed the activity profiles (Fig. 6(a)), with two peaks centered at approximately 120 and 337 °C. For the Ti(3)Si(1) catalyst, only the low temperature peak exhibited an obvious increase, which may be responsible for the increase in catalytic activity due to the presence of SiO_2.

Furthermore, the influences of nitrate must be considered and discussed based on the stability of the species. Whereas the weak bonding of NO_2 at low temperatures enhances the activity, the desorption of NO_2 at higher temperatures results in increased

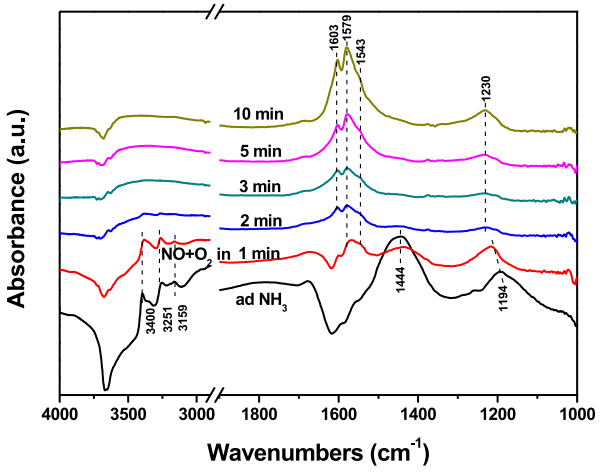

Fig. 8. DRIFTS spectra of the Ti(1)Si(0) catalyst pretreated with 500 ppm NH_3, and then exposed to 500 ppm NO and 3% O_2 at 200 °C.

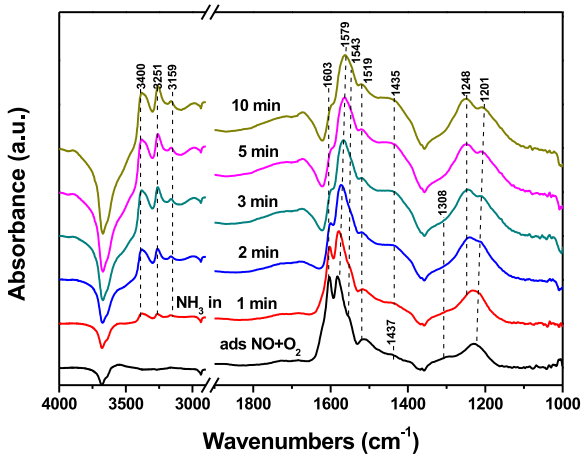

Fig. 9. DRIFTS spectra of Ti(1)Si(0) catalyst pretreated by 500 ppm NO and 3% O_2, and then exposed to 500 ppm NH_3 at 200 °C.

stability, which is unfavorable to the SCR reaction that results from occupying the active sites of the catalysts at low temperature. These species can be assigned to the bridging or bidentate nitrates based on the DRIFTS below (Fig. 7(a) for stability and Fig. 9 for reactivity). The results suggest that unstable nitrates (monodentate or adsorbed NO_2) adsorbed on the surface of the catalysts may improve the SCR reactions, whereas stable surface species (bridging or bidentate nitrate) are less active, especially in the low temperature range.

To further distinguish between the nitrate and nitrite species on the surface of the catalysts, NO + O_2 adsorption/desorption in the temperature range of 50–300 °C are performed on the Ti(1)Si(0) catalyst and further analyzed by IR spectroscopy. As shown in Fig. 7(a), the peak at 1221 cm^{-1} is due to the presence of surface nitrites, whereas the peaks at 1440, 1510 and 1582 cm^{-1} are due to the monodentate, bidentate and bridging nitrates, respectively. In addition, the peak at 1350 cm^{-1} is assigned to the $N_2O_2^{2-}$ species, which are produced by the strong reduction of nitrate or nitrite after the adsorption of NO on CeO_2. Finally, the peak at 1603 cm^{-1} is due to the adsorbed NO_2 [26,32,33]. Nitrite, bidentate nitrate and adsorbed NO_2 content decreased with increasing temperature, whereas the bridging nitrate exhibited a slight increase in the range of 50–200 °C and then a significant decrease at 250 °C and higher temperatures. These findings can be attributed to the transformation of bidentate nitrate to a bridging nitrate at low temperatures, which both remain adsorbed on the catalyst in a stable form until approximately 300 °C. Similar results were observed with other samples (shown in Figure S4) except the Ti(0)Si(1). Fig. 7(b) provides the results from the NO_x adsorption on the Ti(x)Si(y) catalysts at 100 °C. With increasing SiO_2 loading, the band due to surface nitrites shifted to higher wavenumber, whereas the monodentate nitrate increased slightly. In addition, the peaks attributed to bidentate nitrate could no longer be observed, which may be due to the overlap of the large bridging nitrate peaks.

Based on the results above, the reactive NO_x species are nitrite, monodentate nitrate and adsorbed NO_2 species. Indeed, the bridging and bidentate nitrate species are too stable to react with NH_3 species at relative low and mediate temperature. Doping with SiO_2 might promote the presence of surface nitrite and monodentate nitrate, which would increase the SCR performance.

3.5. Reaction mechanism at 200 °C

The Ti(1)Si(0) was first pretreated with NH_3/N_2 for 1 h at 200 °C and then purged with N_2 purging. NO + O_2/N_2 was then introduced into the IR cell and the spectra were recorded as a function of time (Fig. 8). As noted above, NH_3 species bonded to the Lewis (1194, 3000–3500 cm^{-1}) and Brønsted (1444 cm^{-1}) acid sites were observed on the surface of the Ti(1)Si(0) catalyst in the presence of NH_3. When NO + O_2 was introduced, the presence of all NH_3 species decreased significantly within 2 min. Instead of NH_3 signals, peaks attributed to nitrate were observed and remained remarkably strong after 10 min. The results indicate that both Lewis and Brønsted acid sites can participate in the SCR reaction with NO species.

To define the reactive NO_x species, the order of the gas mixture introduced to the IR cell was reversed: the sample was first treated with NO + O_2/N_2 for 1 h at 200 °C, purged with N_2 and treated with NH_3/N_2 (Fig. 9). At this temperature, the nitrate can exist in a stable form on the surface of the catalyst, resulting in a weak peak at 1294 cm^{-1}, which can be attributed to nitrites. When the NH_3 was introduced, the amount of nitrate species slightly decreased, and the nitrites disappeared. Subsequently, peaks attributed to NH_3 species were observed. The results indicate that monodentate nitrate rather than bridging or bidentate nitrate can react with the gaseous or adsorbed NH_3. The disappearance of nitrite can be attributed to the peak overlap with the Lewis acid sites at 1215 cm^{-1} or the reaction with NH_3 species at 200 °C. The reaction mechanism for the Ti(3)Si(1) catalyst was also investigated at 200 °C by in situ IR studies (Figure S5) and the results did not reveal any new mechanism pathway in comparison with the Ti(1)Si(0).

4. Conclusion

Whereas the doping of CeO_2–WO_3/TiO_2 catalyst with SiO_2 increased the reaction rate at relatively low temperatures, excess SiO_2 decreased the catalytic activity at higher temperatures. From a physical perspective, the presence of SiO_2 increased the BET surface area of the catalysts, promoting the dispersion quality of the system, rather than varying the crystal structure of CeO_2 and WO_3 on support. From a chemical perspective, the presence of SiO_2 exhibited a weak influence on the reducibility of the catalysts and also dramatically increased the number of Brønsted acid sites (key acid sites at low temperature). The comparison of NO_x adsorption/desorption properties of Ti(x)Si(y) catalysts revealed that the quantities of nitrite, monodentate nitrates and adsorbed NO_2 correlated well with the SCR activity. Finally, the Ti(1)Si(0) catalyst was used to study the SCR mechanism, and the same behavior was observed with SiO_2 doping. At 200 °C, both Lewis and Brønsted acid sites can react with the nitrite, monodentate nitrate and adsorbed NO_2 species.

Acknowledgments

The authors gratefully acknowledge the financial support of the National High-Tech Research and Development (863) Program of China (2010AA065002 and 2012AA062506) and the Science and Technology Department of Guangdong Province (2011A032303002).

Appendix A. Supplementary data

Supplementary data associated with this article can be found, in the online version, at http://dx.doi.org/10.1016/j.apcatb.2013.04.030.

References

[1] G. Ramis, L. Yi, Catalysis Today 28 (1996) 373–380.
[2] G. Busca, L. Lietti, G. Ramis, F. Berti, Applied Catalysis B – Environmental 18 (1998) 1–36.

[3] M.D. Amiridis, R.V. Duevel, I.E. Wachs, Applied Catalysis B – Environmental 20 (1999) 111–122.
[4] I. Giakoumelou, C. Fountzoula, C. Kordulis, S. Boghosian, Journal of Catalysis 239 (2006) 1–12.
[5] N. Apostolescu, B. Geiger, K. Hizbullah, M.T. Jan, S. Kureti, D. Reichert, F. Schott, W. Weisweiler, Applied Catalysis B – Environmental 62 (2006) 104–114.
[6] Y.J. Kim, H.J. Kwon, I.S. Nam, J.W. Choung, J.K. Kil, H.J. Kim, M.S. Cha, G.K. Yeo, Catalysis Today 151 (2010) 244–250.
[7] J. Morales, A. Caballero, J.P. Holgado, J.P. Espinós, A.R. González-Elipe, Journal of Physical Chemistry B 106 (2002) 10185–10190.
[8] A. Grossale, I. Nova, E. Tronconi, Catalysis Today 136 (2008) 18–27.
[9] M. Colombo, I. Nova, E. Tronconi, Catalysis Today 151 (2010) 223–230.
[10] M.V. Ganduglia-Pirovano, A. Hofmann, J. Sauer, Surface Science Reports 62 (2007) 219–270.
[11] G. Qi, Journal of Catalysis 217 (2003) 434–441.
[12] R. Jin, Y. Liu, Z. Wu, H. Wang, T. Gu, Chemosphere 78 (2010) 1160–1166.
[13] W. Xu, H. He, Y. Yu, Journal of Physical Chemistry C 113 (2009) 4426–4432.
[14] W. Shan, F. Liu, H. He, X. Shi, C. Zhang, Catalysis Today 184 (2012) 160–165.
[15] L. Chen, J. Li, M. Ge, R. Zhu, Catalysis Today 153 (2010) 77–83.
[16] L. Chen, J. Li, M. Ge, L. Ma, H. Chang, Chinese Journal of Catalysis 32 (2011) 836–841.
[17] Y. Peng, J. Li, L. Chen, J. Chen, J. Han, H. Zhang, W. Han, Environmental Science & Technology 46 (2012) 2864–2869.
[18] Y. Peng, Z. Liu, X. Niu, L. Zhou, C. Fu, H. Zhang, J. Li, W. Han, Catalysis Communications 19 (2012) 127–131.
[19] M. Kobayashi, R. Kuma, S. Masaki, N. Sugishima, Applied Catalysis B – Environmental 60 (2005) 173–179.
[20] P.G. Smirniotis, P.M. Sreekanth, D.A. Peña, R.G. Jenkins, Industrial & Engineering Chemistry Research 45 (2006) 6436–6443.
[21] M.A.L. Vargas, M. Casanova, A. Trovarelli, G. Busca, Applied Catalysis B – Environmental 75 (2007) 303–311.
[22] M. Banares, I. Wachs, Journal of Raman Spectroscopy 33 (2002) 359–380.
[23] X. Xia, R. Jin, Y. He, J.F. Deng, H. Li, Applied Surface Science 165 (2000) 255–259.
[24] W. Shan, F. Liu, H. He, X. Shi, C. Zhang, Applied Catalysis B – Environmental 115–116 (2012) 100–106.
[25] M. Galan-Fereres, R. Mariscal, L.J. Alemany, J.L.G. Fierro, J.A. Anderson, Journal of the Chemical Society-Faraday Transactions 90 (1994) 3711–3718.
[26] K.I. Hadjiivanov, Catalysis Reviews 42 (2000) 71–144.
[27] M.A. Centeno, I. Carrizosa, J.A. Odriozola, Applied Catalysis B – Environmental 29 (2001) 307–314.
[28] A.S. Mamede, E. Payen, P. Grange, G. Poncelet, A. Ion, M. Alifanti, V.I. Pârvulescu, Journal of Catalysis 223 (2004) 1–12.
[29] G. Qi, R.T. Yang, R. Chang, Applied Catalysis B – Environmental 51 (2004) 93–106.
[30] C. Ciardelli, I. Nova, E. Tronconi, D. Chatterjee, B. Bandl-Konrad, Chemical Communications 23 (2004) 2718–2719.
[31] P. Forzatti, I. Nova, E. Tronconi, Industrial & Engineering Chemistry Research 49 (2010) 10386–10391.
[32] Z. Wu, B. Jiang, Y. Liu, H. Wang, R. Jin, Environmental Science & Technology 41 (2007) 5812–5817.
[33] L. Chen, J. Li, M. Ge, Environmental Science & Technology 44 (2010) 9590–9596.